PHYSICAL REVIEW A VOLUME 36, NUMBER 4 AUGUST 15, 1987

Optical gain, phase shift, and profile in free-electron lasers

B. Hafizi,* P. Sprangle, and A. Ting†
Naval Research Laboratory, Washington, D.C. 20375-5000
(Received 2 March 1987)

The gain, phase shift, wave-front curvature, and radius of the radiation envelope in a free-electron-laser amplifier are obtained in the small-signal regime. The electron beam is assumed to have a Gaussian density distribution in the transverse direction. Numerical calculations indicate that the radius and curvature of the radiation beam entering a wiggler asymptote to unique spatially constant values after a finite transition region. However, in the asymptotic region the wave fronts are divergent. Analytical expressions for the gain, phase shift, curvature, and spot size are derived. It is shown analytically that small perturbations of the optical waist and curvature about the matched value are spatially damped out, indicating the stability of the matched envelope. When the electron-beam envelope is modulated in space, the optical spot size oscillates with an almost identical wavelength but is delayed in phase. In the case of small-amplitude long-wavelength betatron modulation of the electron-beam envelope, generation of optical sidebands in wave-number space is examined and the effect on the dispersion characteristics of the primary wave is found to be negligible for typical experimental parameters.

I. INTRODUCTION

A well-known feature of the free-electron laser (FEL) is that the refractive index of the medium is a complex function and hence the radiation is amplified and to some extent focused in the vicinity of the electron beam.[1,2] It may then be possible for the electron and radiation beams to interact over an extended length along the wiggler, with the diffractive tendency being compensated by the FEL interaction, thereby enhancing the efficiency of the process.

Considerable progress has been made in studying this process by several authors.[3-8] The purpose of this paper is to apply the formalism of the Gaussian-Laguerre modal source-dependent expansion (SDE) of Ref. 8 to examine the propagation and guiding of the optical wave in an amplifier operating in the exponential gain regime, for a variety of operating conditions.

The plan of this paper is as follows. In Sec. II the formalism of the SDE is employed to obtain the evolution equations for the radius and the curvature for the lowest-order mode of the optical beam, along with the relevant dispersion relation for a Gaussian electron beam driving an FEL amplifier in the small-signal regime. In Sec. III numerical solutions of the single-mode equation for the radius of the optical beam are presented and compared to the result from a multimode truncation of the radiation field. In this case, and for cases not presented herein, the single-mode and multimode results indicate that the radiation-beam profile entering the wiggler asymptotes to a *unique* form after an initial transient. Additionally, the numerical values of the radius of the radiation envelope and of the wave-front curvature are in fair agreement, irrespective of the degree of mode truncation, indicating the usefulness of the single-mode equations. Limiting ourselves to these equations, the electron beam is then allowed to oscillate at the betatron wavelength and the resulting radiation profile is examined. It is found that the optical-beam envelope follows that of the electrons with almost identical wavelength, but retarded in phase. Section IV discusses the results, deriving formulas for the matched radiation-beam profile (i.e., radius and curvature) in terms of the electron-beam and wiggler parameters. It is shown analytically that perturbations of the profile are spatially damped out, consistent with the numerical observations indicating a unique, asymptotic matched radius and curvature. Appendix A presents the necessary details required to derive the source term, for the wave equation, for a planar wiggler and an electron beam with uniform density along the direction of propagation. Appendix B considers the effect of the modulation of the electron beam on the optical wave. Specifically, a simple analysis, taking into account sideband generation, indicates that the dispersion characteristics of the primary wave are only slightly modified for typical experimental parameters. Appendix C presents the details of the stability calculation.

II. MATHEMATICAL FORMULATION

The purpose of the present section is to present the salient features of the source-dependent expansion method[8] so as to fix the notation and for reference in the subsequent sections.

For a planar wiggler, it is appropriate to assume a linearly polarized radiation vector potential

$$\mathbf{A}=\tfrac{1}{2}A(r,\theta,z)\exp\left[i\left(\frac{\omega z}{c}-\omega t\right)\right]\mathbf{e}_x+\text{c.c.}\ ,$$

with angular frequency ω and complex amplitude A. In the slowly-varying-envelope approximation, the wave equation reduces to

$$\left[\frac{1}{r}\frac{\partial}{\partial r}r\frac{\partial}{\partial r}+\frac{1}{r^2}\frac{\partial^2}{\partial\theta^2}+\frac{2i\omega}{c}\frac{\partial}{\partial z}\right]a=S(r,\theta,z)\ , \tag{1}$$

where $a=|e|A/m_0c^2$, and the source function is given by

$$S(r,\theta,z)=-\frac{8\pi|e|}{m_0c^3}\left\{J_x(r,\theta,z)\exp\left[-i\left[\frac{\omega z}{c}-\omega t\right]\right]\right\}_{\rm slow}\ . \tag{2}$$

Here e is the charge on an electron of (rest) mass m_0, $J_x(r,\theta,z)$ is the current density, and $\{\ \}_{\rm slow}$ indicates that only the spatially and temporally slow part of the quantity in braces is to be retained.

The basic premise of the work presented herein is that the radiation field is azimuthally symmetric and the vector potential is expressible as

$$a(r,\theta,z)=\sum_{m=0}^{\infty}a_m(z)D_m(\xi,z)\ , \tag{3}$$

with $D_m=L_m(\xi)\exp\{-[1-i\alpha(z)]\xi/2\}$, where $\xi=2r^2/r_s^2(z)$, $r_s(z)$ is related to the radiation spot size, $\alpha(z)$ is proportional to the curvature of the wave front, and $L_m(\xi)$ is the Laguerre polynomial of order m.

Now, if the transverse profile of the radiation beam is close to a Gaussian, the lowest-order mode is expected to dominate,[3,5,7,8] and, following Ref. 8, it is simple to show that the associated vector potential evolves according to

$$\left[\frac{\partial}{\partial z}+A_0\right]a_0\simeq -iF_0\ , \tag{4}$$

and the spot size and wave-front curvature evolve via

$$\frac{d}{dz}r_s-\frac{2c\alpha}{\omega r_s}=-r_s\left[\frac{F_1}{a_0}\right]_I\ , \tag{5a}$$

$$\frac{d}{dz}\alpha-2(1+\alpha^2)\frac{c}{\omega r_s^2}=2\left[\left[\frac{F_1}{a_0}\right]_R-\alpha\left[\frac{F_1}{a_0}\right]_I\right]\ , \tag{5b}$$

where

$$A_0=\frac{1}{r_s}\frac{d}{dz}r_s+i\left[(1+\alpha^2)\frac{c}{\omega r_s^2}-\frac{\alpha}{r_s}\frac{d}{dz}r_s+\frac{1}{2}\frac{d}{dz}\alpha\right]\ ,$$

the F's are given by the following overlap integral:

$$F_m(z)=\frac{c}{2\omega}\int_0^\infty d\xi\, S(\xi,z)D_m^*(\xi,z)\ , \tag{6}$$

and the label R (I) indicates the real (imaginary) part.

Noting that $L_0(\xi)=1$, the normalized vector potential is seen to be given by [Eq. (3)]

$$a(r,\theta,z)\simeq a_0(z)\exp\left[-[1-i\alpha(z)]\frac{r^2}{r_s^2(z)}\right]\ , \tag{7}$$

where, in the exponential gain, small-signal regime,

$$a_0(z)\simeq a(0)\exp\left[i\int_0^z dz_1[\Delta k(z_1)-i\Gamma(z_1)]\right]\ . \tag{8}$$

Here $a(0)$ is the input signal at $z=0$, and the two components of the refractive index are given by

$$n_z=\left[1+\frac{c\Delta k}{\omega}\right]-i\frac{c}{\omega}\left[\Gamma-r^2\frac{\partial}{\partial z}\frac{1-i\alpha}{r_s^2}\right]\ , \tag{9a}$$

$$n_r=\frac{2cr}{\omega r_s^2}(\alpha+i)\ . \tag{9b}$$

Assuming the electron-beam profile to be given by

$$n_b(z)=n_{b0}\left[\frac{r_{b0}}{r_b(z)}\right]^2\exp\left[-\frac{r^2}{r_b^2(z)}\right]\ , \tag{10}$$

where $r_b(z)$ is the electron-beam radius at z and n_{b0} is the beam density at $r_b(z)=r_{b0}$, the source term in Eq. (1) may be readily evaluated (Appendix A) to obtain

$$S(r,z)=f_B^2\frac{\omega_{b0}^2}{2\gamma^3c^2}\left[\frac{r_{b0}}{r_b(z)}\right]^2\exp\left[-\frac{r^2}{r_b^2}\right]\frac{\omega k_w a_w^2 a}{c(\Delta k-i\Gamma)^2}\ , \tag{11}$$

where the vector potential of the planar wiggler of periodicity $2\pi/k_w$ is given by

$$\mathbf{A}_w=A_w\cos(k_wz)\mathbf{e}_x\ , \tag{12}$$

$$a_w=|e|A_w/m_0c^2\ , \tag{13}$$

γ is the relativistic mass factor, f_B is the usual difference of Bessel functions, $f_B=J_0(\zeta)-J_1(\zeta)$, $\zeta=(1/4)a_w^2/[1+(1/2)a_w^2]$, and

$$\omega_{b0}=(4\pi|e|^2n_{b0}/m_0)^{1/2}$$

is the plasma frequency of the electron beam with density n_{b0}.

Substituting Eqs. (8) and (11) into Eq. (6) and making use of Eqs. (4) and (5), it is simple to show that the equations reduce to

$$\frac{d\alpha}{d(k_wz)}=2(1+\alpha^2)\left[\frac{ck_w}{\omega}\right]\frac{1}{(k_wr_s)^2}+2\left[\left[\frac{F_1}{k_wa_0}\right]_R-\alpha\left[\frac{F_1}{k_wa_0}\right]_I\right]\ , \tag{14a}$$

$$\frac{d(k_wr_s)^2}{d(k_wz)}=4\alpha\left[\frac{ck_w}{\omega}\right]-2\left[\frac{F_1}{k_wa_0}\right]_I(k_wr_s)^2\ , \tag{14b}$$

$$\frac{\Delta k}{k_w}-i\frac{\Gamma}{k_w}+2\left[\frac{ck_w}{\omega}\right]\frac{1-i\alpha}{(k_wr_s)^2}+2\left[\frac{F_1}{k_wa_0}\right]\left[1+\left[\frac{r_b}{r_s}\right]^2\right]=0\ , \tag{14c}$$

where

$$\frac{F_1}{k_wa_0}=f_B^2\left[\frac{\omega_{b0}}{ck_w}\right]^2\left[\frac{r_{b0}}{r_b(z)}\right]^2\frac{a_w^2}{2\gamma^3}\frac{(r_b/r_s)^2}{[1+2(r_b/r_s)^2]^2}\times\left[\frac{\Delta k}{k_w}-i\frac{\Gamma}{k_w}\right]^{-2}\ . \tag{14d}$$

The spatial evolution of the system is governed by the differential system (14a) and (14b) along with the dispersion relation (14c), the solution of which yields $\alpha(z)$, $r_s(z)$, $\Delta k(z)$, and $\Gamma(z)$.

III. NUMERICAL RESULTS

Having obtained the single-mode system of Eqs. (14), it is of interest to determine the extent to which it approximates the general solution in (3). Once it is established that Eqs. (14) provide an adequate representation of the general solution, it is then possible to study a variety of problems of interest by solving a simple set of equations. Briefly, the numerical procedure for solving an initial-value problem is the following. Substituting Eq. (14d) into Eq. (14c) yields a cubic (algebraic) equation for $\Delta k - i\Gamma$ which may be solved, at each z, in terms of $r_s(z)$, $\alpha(z)$, and $r_b(z)$, thus enabling Eqs. (14a) and (14b) to be stepped forward in z. Since in the absence of source terms an input radiation signal diffracts away on the scale length defined by the Rayleigh range z_R,

$$z_R = \left.\frac{\omega r_s^2(z)}{2c}\right|_{z=0}, \tag{15}$$

it is informative to present the numerical results with the distance along the wiggler measured in units of the Rayleigh range. In all the numerical results to be presented, the radiation field is assumed to be in the form of plane waves at the entrance to the wiggler, i.e., $\alpha(z=0)=0$.

A. Case I

To begin with, Fig. 1 shows the results for the following parameters: beam current $I_b=270$ A, $r_{b0}=0.01$ cm, $\gamma=2000$, $2\pi/k_w=10$ cm, $a_w=6.15$, and $r_s(z=0)=0.02$ cm. Noting the factor of $2^{1/2}$ difference between the definition of a_w in Eq. (13) and that in Ref. 4, it is clear from Fig. 1(a) that after a transient oscillation over a distance of about 20 Rayleigh ranges, the radiation spot size approaches a value quite close to that obtained with the two-dimensional FEL code FRED at the Lawrence Livermore National Laboratory (LLNL).[4] We also find that for all the numerical cases examined, a unique, asymptotic spot size is obtained irrespective of the initial optical waist. Figure 1(b) shows the spatial evolution of α, indicating that it, too, approaches a constant value after an initial transient behavior.

The solid curve in Fig. 2 shows the evolution of the $1/e$ width of the radiation amplitude with a five-mode ($m=0,1,2,3,4$) source-dependent expansion calculation using the same set of FEL parameters. The radiation field is represented by Eq. (3) and the source term is given by Eq. (11). With the assumption that the fundamental mode dominates, only the Δk and Γ of $a_0(r,z)$ are involved in the source function and they are obtained from Eqs. (14c) and (14d). It is found that the fundamental mode remains dominant over many Rayleigh lengths. For comparison, the dashed curve in Fig. 2 shows the fundamental mode spot size of Fig. 1(a), and the asymptotic results are seen to differ by about 10%. This suggests that the single-mode system of Eqs. (14) may be regarded as a reasonably accurate simplification of Eq. (3). Henceforth, the results presented pertain to Eqs. (14).

B. Case II

Figure 3 presents the results for a case where the electron beam is not matched, i.e., the envelope of the electron beam is modulated:

$$r_b(z)=r_{b0}+\delta r_b \sin(k_\beta z), \tag{16}$$

where δr_b is the amplitude of the modulation and for simplicity k_β is chosen to be equal to the betatron wave number[9] $k_w a_w/(\sqrt{2}\gamma\beta_z)$, neglecting self-fields.[10] β_z is the beam speed along the wiggler axis normalized to c. The

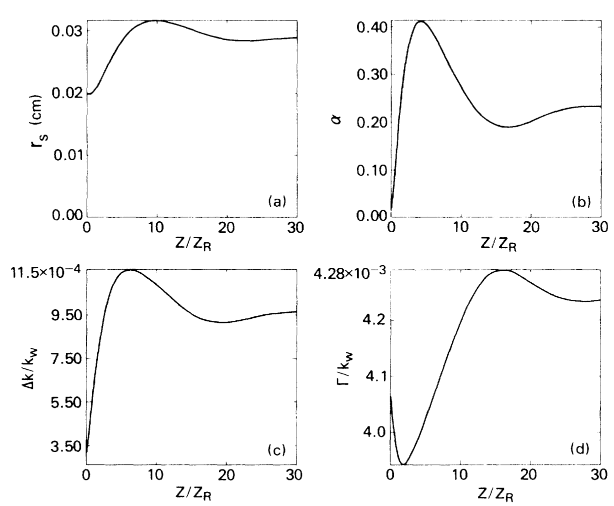

FIG. 1. Spot size (r_s), α, phase shift (Δk), and gain (Γ) vs distance along the wiggler. z is normalized to the Rayleigh range z_R.

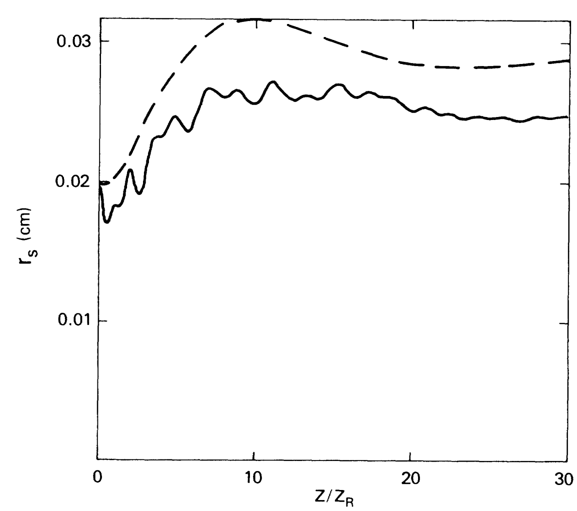

FIG. 2. $(1/e)$ width of the optical field vs distance along the wiggler. Solid curve, five-mode system; dashed curve, one-mode system.

parameters, typical of the Advanced Test Accelerator experiment at LLNL, are $I_b=2$ kA, $r_{b0}=0.3$ cm, $\gamma=100$, $2\pi/k_w=8$ cm, $a_w=1.72$, and $r_s(z=0)=0.35$ cm. (The reader is referred to Refs. 9 and 11 for details.) In Fig. 3, where $\delta r_b/r_{b0}=0.1$, it is observed that the optical spot size follows the modulations in the electron envelope apparently identically. Specifically, a number of cases were examined with $\delta r_b/r_{b0}$ up to 0.4. In all cases the electron and optical beams oscillate with almost identical wavelength, although the radiation beam appears to lag behind in phase. Defining the modulation depth $\Delta=[(r)_{\max}-(r)_{\min}]/[(r)_{\max}+(r)_{\min}]$, it is found from Fig. 3(a) that $\Delta_s=0.087$ whereas, from Eq. (16), $\Delta_b=\delta r_b/r_{b0}=0.1$. Although the modulation depth of the electron beam differs from that of the radiation beam, it is found that Δ_s increases with δr_b.

More generally, allowing for the defocusing effect of self-fields, there is always the possibility of a small-amplitude ripple on the electron-beam envelope and hence on the radiation-beam envelope. In Appendix B, generation of sidebands is considered in a simplified model and found to have, for typical cases, an insignificant effect on the linear dispersion characteristics of the primary optical wave, as implicitly assumed by employing the source term in Eq. (11) in the present case.

IV. ANALYSIS OF RESULTS

One interesting feature of the numerical results is that in all cases the radiation spot size has a unique, asymptotic limit irrespective of the initial value. The asymptotic value of r_s and of α is determined by the fixed points of Eqs. (14a) and (14b), i.e., at the fixed point

$$2(1+\alpha^2)\frac{ck_w}{\omega}\frac{1}{(k_w r_s)^2} + 2\left[\left(\frac{F_1}{k_w a_0}\right)_R - \alpha\left(\frac{F_1}{k_w a_0}\right)_I\right]=0 , \qquad (17a)$$

$$4\alpha\frac{ck_w}{\omega} - 2\left(\frac{F_1}{k_w a_0}\right)_I (k_w r_s)^2 = 0 . \qquad (17b)$$

Combining Eqs. (17a) and (17b) one obtains

$$(1-i\alpha)^2\frac{ck_w}{\omega} + (k_w r_s)^2\left(\frac{F_1}{k_w a_0}\right) = 0 ,$$

which, upon making use of Eq. (14d), yields

$$\Delta k = \frac{k_w^2 r_b \eta^{1/2}}{1+2f}\frac{\alpha}{1+\alpha^2}, \quad \Gamma=\Delta k/\alpha ,$$

where

$$\eta = f_B^2\left(\frac{\omega}{ck_w}\right)\left(\frac{\omega_{b0}}{ck_w}\right)^2\left(\frac{r_{b0}}{r_b}\right)^2\frac{a_w^2}{2\gamma^3} ,$$

and $f=(r_b/r_s)^2$ is the filling factor. Substituting the expressions for Δk and Γ into the dispersion relation (14c), one obtains

$$\alpha=[f/(3f+2)]^{1/2} ,$$

$$r_s = \frac{(\gamma/\nu)^{1/4}}{2^{3/4}k_w\gamma f_B^{1/2}}\frac{(1+a_w^2/2)^{3/4}}{a_w^{1/2}}\frac{f^{1/4}(1+2f)^{3/2}}{(1+3f/2)^{3/4}} ,$$

where $\nu=(\omega_{b0}r_{b0}/2c)^2$ is Budker's parameter. These expressions may be used to obtain the asymptotic spot size for a given filling factor, and then one obtains the corresponding electron-beam radius via $r_b=r_s f^{1/2}$. To avoid complications arising at the outer edges of the optical beam, where the field amplitude is small, typically a filling factor $f \lesssim \frac{1}{2}$ is appropriate. It is also possible to rearrange the expression for r_s to obtain

$$f^3+f^2+(\tfrac{1}{4}-\tfrac{3}{2}q)f-q=0 ,$$

where

$$q=\left[a_w^2\left(\frac{2f_B^2}{\gamma/\nu}\right)\left(\frac{\gamma r_b k_w}{2}\right)^4\right]^{1/3}\frac{1}{1+a_w^2/2} .$$

The cubic equation for f may be solved to obtain an explicit expression for r_s. Noting that the sum and the product of the three roots of the cubic equal -1 and q, respectively, it follows that there is a unique, real value for the asymptotic spot size r_s.

To examine stability, it is convenient to define

$$Y \equiv \frac{\Delta k}{k_w} - i\frac{\Gamma}{k_w} ,$$

and subsititute Eq. (14d) into Eq. (14c) to obtain the local dispersion relation

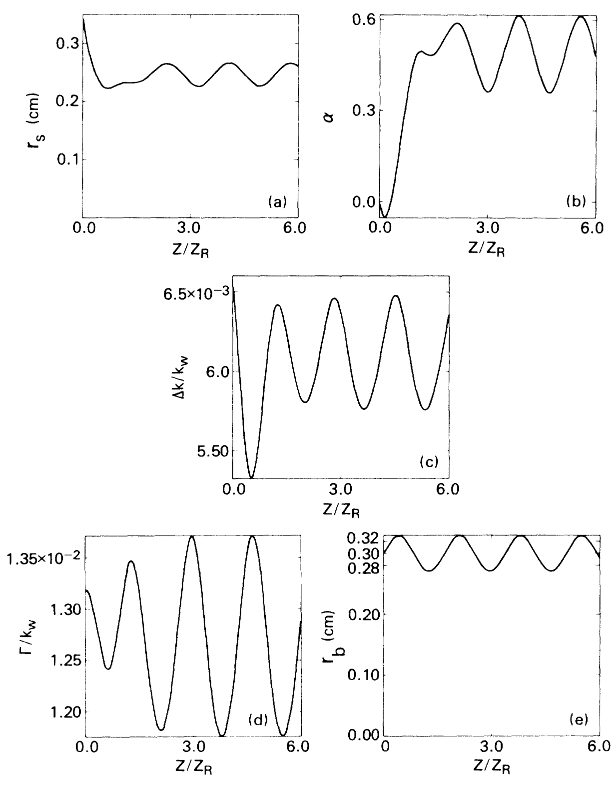

FIG. 3. Spot size (r_s), α, phase shift (Δk), gain (Γ), and radius of electron beam (r_b) vs distance along wiggler.

$$Y^3+2\left[\frac{ck_w}{\omega}\right]\frac{1-i\alpha}{(k_w r_s)^2}Y^2=-2\frac{ck_w}{\omega}\eta\left[\frac{r_b}{r_s}\right]^2 \times\frac{1+(r_b/r_s)^2}{[1+2(r_b/r_s)^2]^2}\ , \quad (18)$$

which may be solved iteratively. It turns out that for the parameters of case I, at the lowest order, the right-hand side balances the quadratic term on the left. The relevant root, with Δk, $\Gamma>0$, may be substituted into Eq. (14d) to obtain, for $\alpha>0$,

$$\frac{F_1}{k_w a_0}\simeq\frac{-ck_w}{\omega}\frac{1-i\alpha}{(k_w r_s)^2+(k_w r_b)^2}-\frac{1}{2}\left[\frac{\eta}{2(1+\alpha^2)}\right]^{1/2}\frac{\alpha-i[1+(1+\alpha^2)^{1/2}]}{[1+(1+\alpha^2)^{1/2}]^{1/2}}\frac{(k_w r_s)^2}{(k_w r_s)^2+2(k_w r_b)^2}\frac{(k_w r_s)(k_w r_b)}{[(k_w r_s)^2+(k_w r_b)^2]^{1/2}}\ . \quad (19)$$

Perturbing Eqs. (14a) and (14b) about the fixed point and making use of Eq. (19), it is simple to show that the perturbation is spatially damped, thus indicating the stability of the fixed point. The algebraic details are relegated to Appendix C.

Another aspect of the results which is of interest pertains to the nature of the phase fronts and the flux of optical power in the asymptotic region. From Eqs. (7) and (8) it is simple to check that, in differential form, the surfaces of constant phase are given by $(\omega/c+\Delta k)\delta z + (2r\alpha/r_s^2)\delta r=0$, and hence, noting that Δk, $\alpha>0$, the wave fronts are divergent in the direction of propagation. Consistent with this, there is a nonvanishing transverse component of the Poynting flux. Specifically, for $r/r_s \lesssim 1$ the ratio of flux of optical energy in the transverse direction to that along the z axis is $\sim \alpha r/kr_s^2 \ll 1$.

V. CONCLUSION

Based on the results presented herein, the simplicity and accuracy of the single-mode Gaussian-Laguerre approximation to the solution of Maxwell's equations have been demonstrated. It is shown that, in the exponential gain regime of operation of an FEL amplifier, there is a unique, asymptotic spot size for the radiation beam irrespective of that at the entrance of the wiggler. There is, however, a transverse flux of optical power. It is shown analytically that the asymptotic profile (i.e., the radius and the curvature at large z) is stable to small-amplitude perturbations. With a spatially modulated electron-beam envelope, that of the optical beam is found to oscillate on the same spatial scale.

ACKNOWLEDGMENTS

Discussions with Dr. W. P. Marable and Dr. C. M. Tang are gratefully acknowledged. This work was sponsored by U.S. Army Strategic Defense Command.

APPENDIX A: SOURCE TERM

In this appendix, the details of the evaluation of the source term S in Eq. (11) are presented.

The FEL source current, $J_x(r,\theta,z)$ in a linear wiggler is given by

$$J_x(r,\theta,z)=-|e|\,\delta n_b(r,\theta,z)v_x =\frac{-|e|^2\delta n_b e^{-ik_w z}}{2\gamma m_0 c}A_w+\text{c.c.}\ ,$$

where δn_b is the perturbed beam density and the relation $v_x \simeq v_w = |e|\,A_w\cos(k_w z)/\gamma m_0 c$ has been used. Equation (2) can then be written as

$$S(r,\theta,z)=\left[\frac{4\pi|e|^2\delta n_b a_w}{\gamma m_0 c^2}e^{-i[(k+k_w)z-\omega t]}\right]_{\text{slow}}\ , \quad (A1)$$

where $k=\omega/c$.

The perturbed beam density can be evaluated from the continuity equation

$$\frac{d\delta n_b}{dt}=-n_b\frac{\partial\delta v_z}{\partial z}\ , \quad (A2)$$

and the equation of motion in the z direction,

$$\frac{dv_z}{dt}=-\frac{|e|}{\gamma m_0}\left[\frac{v_x B_y}{c}-\frac{v_z(v_x E_x)}{c^2}\right]\ , \quad (A3)$$

where electron self-field effects are neglected. Taking the convective time derivative of Eq. (A2), and incorporating the linearized version of Eq. (A3), one can arrive at the following equation for the perturbed beam density:

$$\frac{d^2\delta n_b}{dt^2}=\frac{-|e|n_b}{\gamma m_0}\frac{\partial}{\partial z}\left[\frac{\partial}{\partial z}+\frac{v_z}{c^2}\frac{\partial}{\partial t}\right]\Phi_{\text{pond}}\ , \quad (A4)$$

where

$$\Phi_{\text{pond}}=\frac{-|e|\,A_w A}{4\gamma m_0 c^2}e^{i[(k+k_w)z-\omega t]}+\text{c.c.}$$

With the assumption that $A(r,\theta,z)$ is a slowly varying function of z, i.e., $|\partial\ln A/\partial z| \ll k_w \ll k$, Eq. (A4) becomes

$$\frac{d^2\delta n_b}{dt^2}=\frac{|e|^2 n_b A_w A}{2\gamma^2 m_0^2 c^2}k_w k e^{i[(k+k_w)z-\omega t]}+\text{c.c.}\ , \quad (A5)$$

where the resonance condition $\omega=v_z(k+k_w)$ is used.

For a near-Gaussian radiation field in the exponential gain regime,

$$A(r,\theta,z) \simeq A_0(r,\theta,z) = A_0(0)\exp\left[i\int_0^z [\Delta k(z_1) - i\Gamma(z_1)]dz_1 - [1 - i\alpha(z)]\frac{r^2}{r_s^2(z)}\right]$$

and assuming that Δk, Γ, α and r_s are slowly varying functions of z, Eq. (A5) can be integrated immediately to give

$$\delta n_b = \frac{|e|^2 n_b A_w A k k_w}{2\gamma^2 m_0^2 c^4(\Delta k - i\Gamma)^2} e^{i[(k+k_w)z-\omega t]} + \text{c.c.} \tag{A6}$$

When Eq. (A6) is substituted into Eq. (A1), taking into account the usual difference of Bessel functions for a planar wiggler, and Eq. (10) for the beam profile, the source function in Eq. (1) is then given by Eq. (11).

APPENDIX B: SIDEBAND GENERATION

In this appendix generation of sidebands to the primary optical wave, due to the spatial modulation of the electron beam, is analyzed. It is to be emphasized that the following analysis is intended merely to show that the dispersion characteristics of the primary optical wave are only slightly modified $[\sim(\delta N_0/N_0)^2]$ for typical experimental parameters, as implicitly assumed in applying the results of Appendix A to the case of a modulated electron beam in Sec. III. The development of the linear theory herein generalizes that of Sprangle *et al.*,[12] to which reference should be made for further details.

The form of the vector potential of a planar wiggler employed in this appendix is slightly different than that given by Eq. (12),

$$\mathbf{A}_w \simeq A_w[\exp(ik_w z) - \text{c.c.}]\mathbf{e}_x ,$$

where A_w is purely imaginary, and that of the linearly polarized radiation field is taken to be of the form

$$\mathbf{A} = [A_+\exp(ik_+z - i\omega t) + A_-\exp(ik_-z - i\omega t) + A_0\exp(ikz - i\omega t) + \text{c.c.}]\mathbf{e}_x ,$$

where it is assumed that the electron density, modulated at the betatron wavelength $2\pi/k_\beta$, has the simple form

$$n_0 = N_0 + \frac{\delta N_0}{2}[\exp(ik_\beta z) + \text{c.c.}] ,$$

with $k_\beta \ll k_w \ll k$, and $k_+ = k + k_\beta$, $k_- = k - k_\beta$.

Following Ref. 12, the wave equation is found to be

$$\left[\frac{\partial^2}{\partial z^2} - \frac{1}{c^2}\frac{\partial^2}{\partial t^2} - \frac{\omega_b^2}{\gamma_0 c^2}\right]\mathbf{A} = \frac{4\pi|e|^2}{\gamma_0 m_0 c^2}\delta n\,\mathbf{A}_w ,$$

where γ_0 is the relativistic factor in the absence of the radiation field, $\omega_b = (4\pi n_0|e|^2/m_0)^{1/2}$, and δn is the density perturbation caused by the radiation. Note that the velocity v_{z0} along the wiggler axis is not affected by the betatron oscillation and hence γ_0, to lowest order in $|eA_w/\gamma_0 m_0 c^2|^2$, is not a function of z. Defining the ponderomotive potential

$$\Phi_{\text{pond}} = \frac{-|e|}{\gamma_0 m_0 c^2}\mathbf{A}_w\cdot\mathbf{A} ,$$

the momentum, continuity, and Poisson's equations may be combined to obtain

$$\frac{d^2}{dt^2}\delta n - \frac{v_{z0}}{n_0}\left[\frac{\partial n_0}{\partial z}\right]\frac{d}{dt}\delta n + \frac{4\pi n_0|e|^2}{m_0\gamma_0\gamma_z^2}\delta n + \frac{|e|}{m_0\gamma_0\gamma_z^2}\left[\frac{\partial n_0}{\partial z}\right]\frac{\partial\Phi}{\partial z} = \frac{-|e|}{m_0\gamma_0}\frac{\partial}{\partial z}n_0\left[\frac{\partial}{\partial z} + \frac{v_{z0}}{c^2}\frac{\partial}{\partial t}\right]\Phi_{\text{pond}} , \tag{B1}$$

where $\gamma_z = (1 - v_{z0}^2/c^2)^{-1/2}$, Φ is the scalar potential, and terms such as $\partial^2 n_0/\partial z^2$, which are on the order of k_β^2, have been neglected.

Writing $k_+ = k + k_\beta$, $k_- = k - k_\beta$,

$$\delta n = \{\delta n_+\exp[i(k_+ + k_w)z - i\omega t] + \delta n_-\exp[i(k_- + k_w)z - i\omega t] + \delta n_0\exp[i(k + k_w)z - i\omega t] + \text{c.c.}\} ,$$

noting that, on the left-hand side of Eq. (B1), the ratio of the fourth to the third term is on the order of $k_\beta/k \ll 1$, one finds that

$$\begin{bmatrix} m_{11} + \epsilon^2 a_- & \epsilon m_{12} & m_{13} \\ \epsilon m_{21} & m_{22} + \epsilon^2 a_{22} & \epsilon m_{23} \\ m_{31} & \epsilon m_{32} & m_{33} + \epsilon^2 a_+ \end{bmatrix}\begin{bmatrix} A_+ \\ A_0 \\ A_- \end{bmatrix} = 0 ,$$

where $\epsilon = (\delta N_0/2N_0)$ and $m_{13}, m_{31} = O(\epsilon^2)$. It is then simple to show that, correct to $O(\epsilon^2)$, the dispersion relation is given by

$$m_{22} - \left[\frac{\delta N_0}{2N_0}\right]^2\left[\frac{m_{32}m_{23}}{m_{33}} + \frac{m_{12}m_{21}}{m_{11}}\right] + \left[\frac{\delta N_0}{2N_0}\right]^2\left[a_{22} + m_{22}\left[\frac{a_+}{m_{33}} + \frac{a_-}{m_{11}}\right]\right] = 0 ,$$

where

$$m_{22} = m_{22}(k) \equiv \left[[\omega - (k + k_w)v_{z0}]^2 - \frac{\omega_{b0}^2}{\gamma_0\gamma_z^2}\right] \times \left[k^2 - \frac{\omega^2}{c^2} + \frac{\omega_{b0}^2}{\gamma_0 c^2}\right] - \frac{2\omega_{b0}^2}{\gamma_0^3}k k_w a_w^2 ,$$

is the usual matrix element for the primary wave, $m_{11} = m_{22}(k_+)$, $m_{33} = m_{22}(k_-)$,

$$m_{12}=m_{12}(k_+,k,k_\beta)$$
$$=\frac{\omega_{b0}^2}{\gamma_0 c^2}\left[[\omega-(k_+ +k_w)v_{z0}]^2-\frac{\omega_{b0}^2}{\gamma_0\gamma_z^2}\right]$$
$$+\left[k_\beta v_{z0}[\omega-(k+k_w)v_{z0}]-\frac{\omega_{b0}^2}{\gamma_0\gamma_z^2}\right]$$
$$\times\left[k^2-\frac{\omega^2}{c^2}+\frac{\omega_{b0}^2}{\gamma_0 c^2}\right]-\frac{2\omega_{b0}^2}{\gamma_0^2}k_+k_w a_w^2\ ,$$
$$m_{21}=m_{12}(k,k_+,-k_\beta),\quad m_{23}=m_{12}(k,k_-,k_\beta)\ ,$$
$$m_{32}=m_{12}(k_-,k,-k_\beta)\ ,$$
$$a_{22}=-\frac{2\omega_{b0}^4}{\gamma_0^2\gamma_z^2c^2}+\frac{2\omega_{b0}^2k_\beta^2v_{z0}^2}{\gamma_0 c^2}\ ,$$
$$a_\mp=\frac{\omega_{b0}^2}{\gamma_0 c^2}\left[k_\beta v_{z0}[\omega-(k+k_w)v_{z0}]\mp\frac{\omega_{b0}^2}{\gamma_0\gamma_z^2}\right]\ ,$$

and $\omega_{b0}=(4\pi e^2N_0/m_0)^{1/2}$. Note that with the definition chosen for A_w in this appendix, $a_w^2=(eA_w/m_0c^2)^2<0$.

To proceed along the lines of Ref. 12, it is convenient to write

$$m_{22}=M_{22}+C_{22}\ ,$$

where

$$M_{22}=\left[[\omega-(k+k_w)v_{z0}]^2-\frac{\omega_{b0}^2}{\gamma_0\gamma_z^2}\right]\times\left[k^2-\frac{\omega^2}{c^2}+\frac{\omega_{b0}^2}{\gamma_0c^2}\right]\ ,$$

and

$$C_{22}=\frac{-2\omega_{b0}^2}{\gamma_0^3}kk_wa_w^2$$

is the "coupling" term. The dispersion relation then becomes

$$\left[1+\left[\frac{\delta N_0}{2N_0}\right]^2\left[\frac{a_+}{m_{33}}+\frac{a_-}{m_{11}}\right]\right]M_{22}=-\left[1+\left[\frac{\delta N_0}{2N_0}\right]^2\left[\frac{a_+}{m_{33}}+\frac{a_-}{m_{11}}\right]\right]C_{22}+\left[\frac{\delta N_0}{2N_0}\right]^2\left[\frac{m_{12}m_{21}}{m_{11}}+\frac{m_{32}m_{23}}{m_{33}}-a_{22}\right]\ . \tag{B2}$$

M_{22} yields the dispersion relation for uncoupled electromagnetic and space-charge waves. The right-hand side of Eq. (B2) introduces the FEL interaction and coupling to sidebands, and its effect is included iteratively. At the lowest order, $M_{22}=0$ for some (ω,k). Substituting in the right-hand side, the second set of terms vanishes; the term proportional to C_{22} survives.

Substantial modification of this dispersion relation is expected if

$$1+\left[\frac{\delta N_0}{2N_0}\right]^2\left[\frac{a_+}{m_{33}}+\frac{a_-}{m_{11}}\right]\ll 1$$

i.e., if

$$\frac{\delta N_0}{N_0}\sim 2k_\beta c\omega_{b0}^{-3/2}(2kv_{z0})^{1/2}\gamma_z^{1/2}\gamma_0^{3/4}\ .$$

For typical experimental parameters, the right-hand side of this equation exceeds unity, whereas $\delta N_0/N_0\ll 1$, implying the insignificance of the effect of modulation on the dispersion relation.

APPENDIX C: STABILITY ANALYSIS

The purpose of this appendix is to establish the stability of the fixed point (r_s,α) of Eqs. (14).

Perturbing Eqs. (14a) and (14b) about the fixed point and making use of Eq. (19), it is seen that the perturbation evolves according to

$$\frac{d}{d(k_wz)}\begin{bmatrix}\delta\alpha\\ \delta x\end{bmatrix}=2\begin{bmatrix}a_{11}&a_{12}\\ a_{21}&a_{22}\end{bmatrix}\begin{bmatrix}\delta\alpha\\ \delta x\end{bmatrix}\ ,$$

where $x=(k_wr_s)^2$, $y=(k_wr_b)^2$,

$$a_{11}=\frac{-\alpha(ck_w/\omega)}{x+y}+X_I+\frac{\partial}{\partial\alpha}(X_R-\alpha X_I)\ ,$$
$$a_{12}=\frac{-(1+\alpha^2)(ck_w/\omega)y(2x+y)}{x^2(x+y)^2}+\frac{\partial}{\partial x}(X_R-\alpha X_I)\ ,$$
$$a_{21}=\frac{xX_I}{\alpha}-x\frac{\partial}{\partial\alpha}X_I\ ,$$
$$a_{22}=-\frac{\alpha(ck_w/\omega)}{(x+y)^2}-\frac{\partial}{\partial x}(xX_I)\ ,$$

and

$$X=-\tfrac{1}{2}\left[\frac{\eta}{2(1+\alpha^2)}\right]^{1/2}\frac{\alpha-i[1+(1+\alpha^2)^{1/2}]}{[1+(1+\alpha^2)^{1/2}]^{1/2}}\times\frac{x}{x+2y}\left[\frac{xy}{x+y}\right]^{1/2}\ . \tag{C1}$$

Assuming that $\delta\alpha,\delta x\sim\exp(\lambda k_wz)$, one finds that

$$\lambda=-\left[\frac{\alpha(ck_w/\omega)(x+2y)}{(x+y)^2}+S_2+S_1\right]\pm\left[\left[\frac{-\alpha(ck_w/\omega)x}{(x+y)^2}+S_2-S_1\right]^2-S_3\right]^{1/2}\ ,$$

where

$$S_1=-\frac{\partial X_R}{\partial\alpha}+\alpha\frac{\partial X_I}{\partial\alpha}\ ,$$
$$S_2=\frac{\partial}{\partial x}(xX_I)\ ,$$
$$S_3=-4x\left[\frac{X_I}{\alpha}-\frac{\partial X_I}{\partial\alpha}\right]\left[\frac{-(1+\alpha^2)(ck_w/\omega)y(y+2x)}{x^2(x+y)^2}+\frac{\partial}{\partial x}(X_R-\alpha X_I)\right]\ .$$

(Note that all the variables in this appendix are evaluated at the fixed point.) Making use of Eq. (C1), it is simple to show that $X_I/\alpha - \partial X_I/\partial\alpha > 0$, $\partial(X_R - \alpha X_I)/\partial x < 0$, whence $S_3 > 0$ and hence, noting that $S_2 + S_1 > 0$, and that the perturbation solution for Eq. (18) implies $S_1 < \alpha(ck_w/\omega)/(x+y)$, one finds that $\mathrm{Re}\lambda < 0$, thus indicating the stability of the fixed point to small-amplitude perturbations.

---

*Permanent address: Science Applications Intl. Corp., McLean, VA 22102.

†Permanent address: Berkeley Research Assoc., Inc., Springfield, VA 22150.

[1]N. M. Kroll, P. L. Morton, and M. N. Rosenbluth, IEEE J. Quantum Electron. **QE-17**, 1436 (1981).

[2]P. Sprangle and C. M. Tang, Appl. Phys. Lett. **39**, 677 (1981).

[3]G. T. Moore, Nucl. Instrum. Methods Phys. Res. A **239**, 19 (1985).

[4]E. T. Scharlemann, A. M. Sessler, and J. S. Wurtele, Phys. Rev. Lett. **54**, 1925 (1985).

[5]G. T. Moore, Nucl. Instrum. Methods, Phys. Res. A **250**, 381 (1986).

[6]J. E. LaSala, D. A. G. Deacon, and E. T. Scharlemann, Nucl. Instrum. Methods, Phys. Res. A **250**, 389 (1986).

[7]M. Xie and D. A. G. Deacon, Nucl. Instrum. Methods, Phys. Res. A **250**, 426 (1986).

[8]P. Sprangle, A. Ting and C. M. Tang, Phys. Rev. Lett. (to be published); Phys. Rev. A (to be published).

[9]E. T. Scharlemann, J. Appl. Phys. **58**, 2154 (1985).

[10]E. P. Lee and R. K. Cooper, Part. Accel. **7**, 83 (1976).

[11]D. Prosnitz, and A. Szoke and V. K. Neil, Phys. Rev. A **24**, 1436 (1981).

[12]P. Sprangle, C. M. Tang and C. W. Roberson, Nucl. Instrum. Methods, Phys. Res. A **239**, 1 (1985).